Sensors and Materials, Vol. 15, No. 3 (2003) 147–154
MYU Tokyo

S & M 0516

Effect of Operating Temperature on Electrical and Thermal Properties of Microbolometer Infrared Sensors

Gamani Karunasiri*, M. V. S. Ramakrishna[1] and P. Neuzil[2]

[1]Department of Physics, Naval Postgraduate School, Monterey, CA 93943, USA
Department of Electrical and Computer Engineering, National University of Singapore
Singapore 119260
[2]Institute of Microelectronics, 11 Science Park Road, Singapore 117685

(Received October 15, 2002; accepted March 10, 2003)

Key words: microbolometer, thermal conductance, heat capacitance, temperature dependence

The electrical and thermal parameters of microbolometer infrared sensors play an important role in determining the ultimate sensitivity of detection. This paper describes in detail the effect of varying the operating temperature (80–300 K) on the thermal and electrical properties of microbolometer infrared detectors using Ti resistive sensor elements. In the experiment, two microbolometers with different thermal conductances were employed. The parameters studied include the temperature coefficient of resistance (TCR), thermal conductance and thermal mass (heat capacitance). The measurements show that the heat capacitance increases linearly with operating temperature while the thermal conductance increases linearly at low temperatures (< 250 K) and then rapidly increases. The rapid increase in thermal conductance at elevated temperatures is mainly due to the radiated heat loss which may limit the performance of microbolometer sensors at high ambient temperatures.

1. Introduction

This decade has witnessed the emergence of thermal detectors as a suitable choice for the detection of infrared radiation[1–5] owing to the advances in micromachining technology. In contrast to conventional photon detectors, thermal detectors can be operated at room temperature. Three of the most common thermal detectors are microbolometers,[1–3] thermopiles[4] and pyroelectric detectors.[5] In addition, high-sensitivity thermal detectors

*Corresponding author, e-mail address: karunasiri@nps.navy.mil

based on microcantilevers have also been fabricated recently.[6] Microbolometers are the most commonly used sensors in thermal imaging arrays due to their high responsivity and ability to operate without mechanical chopping of the incident infrared radiation. The choice of sensor material, the design employed and the operating conditions determine the sensitivity of microbolometers. These requirements are often conflicting and thus careful balancing is required to optimize the relevant parameters. For example, the sensor should have low thermal conductance and low thermal mass (heat capacitance). It is also necessary to use a sensing element with a high temperature coefficient of resistance (TCR) for enhancing the responsivity. However, the low thermal conductance increases the thermal time constant, which limits the operating speed. In addition, these parameters depend on operating conditions such as ambient pressure and temperature. Thus, for example, the operation of an uncooled camera without a thermoelectric (TE) temperature stabilizer would be different depending on whether it is used in the Arctic or an Equatorial region. It is important to take these variations into account in the design of microbolometers in order to optimize the performance under varying operating conditions. However, very little literature is available to date on the influence of ambient conditions on the device parameters. This paper presents the results of a study on the effect of substrate temperature on the electrical and thermal parameters of microbolometers with Ti sensing elements.

The thermal parameters of a microbolometer can be extracted by measuring the increase of its resistance as a function of time in response to a DC bias.[7] This can be conveniently achieved by placing the microbolometer on one arm of a Wheatstone bridge as schematically shown in Fig. 1. Under a constant applied bias (V_B) across the bridge, resistance of the microbolometer increases with time due to self-heating,[7] which in turn, offsets the bridge producing an output voltage. If the values of three reference resistors are adjusted to be the same as that of the ambient resistance of the microbolometer (R_o) then the self-heating power generated in the microbolometer, P_{SH}, is approximately given by[7]

$$P_{SH} \approx \frac{V_B^2}{4R_o}. \tag{1}$$

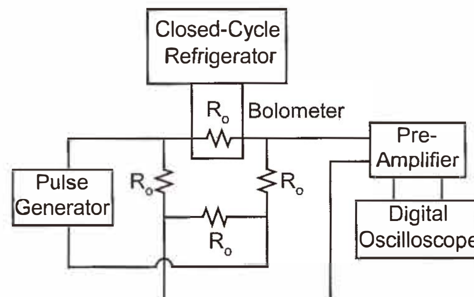

Fig. 1. Experimental setup used for the measurement of electrical and thermal parameters. The reference resistors are selected to have values nearly the same as the microbolometer resistance (R_o) at each temperature.

The above expression is valid only if $\alpha\Delta T << 1$, where α is the TCR of the resistive element and ΔT is the temperature change of the microbolometer due to self-heating. The output voltage, V_{out}, initially rises with a rate determined by the thermal time constant and then saturates as the heat loss balances the self-heating power.[7] The saturated value of the output voltage, V_{sat}, depends on the thermal conductance, G, which can be written as[7]

$$V_{sat} = \frac{\alpha V_B^3}{16 R_o G}, \tag{2}$$

where α is the TCR of the Ti sensing element, R_o is thc ambient resistance of the microbolometer as well as the three reference resistors and V_B is the amplitude of the voltage pulse applied to the bridge. Note that eq. (2) is valid only when all the resistors in the bridge are nearly the same (symmetric bridge) at each temperature before applying the voltage pulse. The temperature dependence of TCR can be determined by measuring the microbolometer resistance as a function of temperature. The TCR is then extracted using the formula

$$\alpha = \frac{1}{R}\frac{dR}{dT}\bigg|_{T=T_S}, \tag{3}$$

where T_s is the substrate temperature.

In addition, the thermal mass, H, can be obtained from the slope of the output voltage vs. time in the linear region ($t << \tau$), which is given by[7]

$$V_{sat} \approx \frac{\alpha V_B^3}{16 R_o H} t. \tag{4}$$

2. Experimental

In the experiment, two microbolometers with nearly the same thermal masses and different thermal conductances were employed to probe the heat loss via radiation in addition to the temperature dependence of thermal parameters. Figures 2(a) and 2(b) show the optical micrographs of the two microbolometers (MB_1 and MB_2) having small and large thermal conductances, respectively. The thermal masses of the two microbolometers were designed to be nearly the same. The fabrication process started with the deposition and patterning of a polysilicon sacrificial layer on a 6" silicon wafer, followed by the plasma-enhanced chemical vapor deposition (PECVD) of a 500-nm-thick silicon nitride membrane. Subsequently, aluminum was sputtered and patterned for use as bond pads. A 60-nm-thick Ti sensing meander line was sandwiched between two layers of 15-nm-thick TiN on the nitride membrane. The entire structure was passivated using a second layer of PECVD silicon nitride. Plasma etching was then used to create openings for subsequent

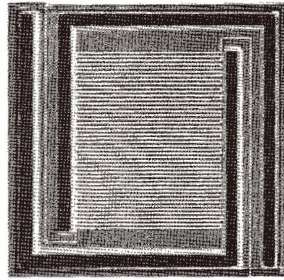

(a)

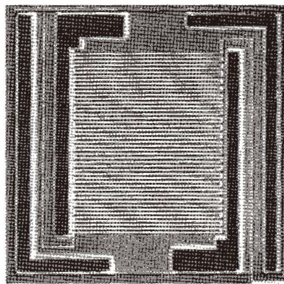

(b)

Fig. 2. Micrographs of (a) MB_1 (low thermal conductance) and (b) MB_2 (high thermal conductance). The total area of each microbolometer is approximately 200×200 μm^2 with an active membrane area of approximately 110×160 μm^2.

micromachining, which was accomplished using a solution of tetra methyl ammonium hydroxide (TMAH) doped with silicon.(6) The active area of the membrane after micromachining is approximately 110×160 μm^2 (see Fig. 2) and has a room temperature resistance of approximately 28 kΩ.

The electrical and thermal parameters in the temperature range 80–294 K were measured by placing the microbolometers in a closed-cycle refrigerator as schematically shown in Fig 1. The pressure inside the cryostat was maintained below 10^{-5} Torr during the experiment in order to eliminate the convective heat loss which is usually the dominant heat-loss mechanism of microbolometers under ambient pressure.(8) The device was covered with a cold shield to ensure that the ambient temperature closely followed that of the substrate. At each substrate temperature, the three external resistors in the bridge were adjusted to balance it against the change in microbolometer resistance with temperature. Table 1 summarizes the measured electrical and thermal parameters of the two microbolometers at room temperature (294 K).

Table 1
Comparison of parameters for MB_1 and MB_2 measured at room temperature (294 K).

	MB_1	MB_2
Resistance	27.9 kΩ	27.8 kΩ
TCR	0.3 %/K	0.3 %/K
Thermal Conductance	3.5×10^{-7} W/K	2.9×10^{-6} W/K
Thermal Mass	4.9×10^{-8} J/K	4.6×10^{-8} J/K

3. Electrical Properties

The measured resistance of MB_2 as expected shows a linear dependence with substrate temperature (solid triangles in Fig. 3) and estimated TCR using eq. (3) has a $1/R$ dependence since dR/dT is nearly independent of temperature as shown by the solid squares in Fig. 3. The bulk TCR of titanium[9] is about 0.38 % while that of the thin film is found to be about 0.3 % at 294 K. The TCR of a thin metal film resistor depends on several factors such as the deposition technique used, the grain size, the annealing temperature and the composition. In addition, the large surface to volume ratio associated with thin film resistors results in higher surface scattering, which is relatively temperature independent. These factors contribute to the lower TCR observed for the thin film as compared with the published[9] TCR for bulk Ti.

4. Thermal Properties

In order to determine the thermal parameters as a function of temperature, the output voltage of the bridge was measured at a set of temperatures by applying a voltage pulse longer than the thermal time constant of the microbolometers.[7] Figure 4 shows the measured output voltage of the bridge for MB_2 at a set of temperatures in the 80–294 K range. The voltage pulse amplitude (V_B) applied to the bridge was reduced as the temperature was decreased to ensure that the membrane temperature did not rise appreciably above that of the substrate (i.e., $\alpha\Delta T << 1$). This condition is necessary to ensure the validity of eqs. (2) and (4) which is particularly important at low temperatures where the smaller microbolometer resistance can generate a large amount of Joule heating[10] and hence, a large temperature rise.

The thermal conductances of the microbolometers were determined using the measured values of the saturated voltages as given in eq. (2), and the results are shown in Fig. 5. It can be seen that for MB_2 the thermal conductance increases linearly in the entire temperature range, while for MB_1 it remains linear only in the low-temperature region (< 250 K) and rapidly increases as the temperature nears ambient. The linear increase in thermal conductance can be attributed to the known increase in membrane phonon density with temperature which enhances the thermal conductivity through the legs. In addition to the thermal conductance through the legs, the increase of membrane temperature (during biasing or due to incident IR) relative to the substrate causes heat loss via radiation. This component of thermal conductance, G_{rad}, is obviously a function of substrate temperature,

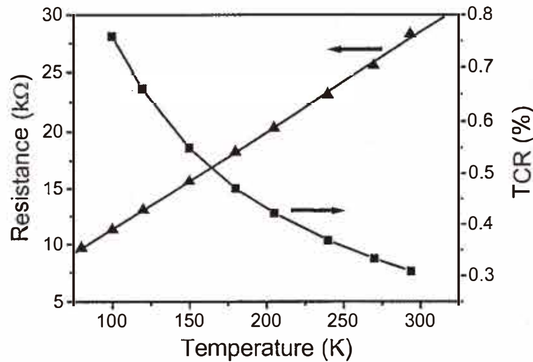

Fig. 3. Measured resistance (solid triangles) and TCR (solid squares) as a function of temperature.

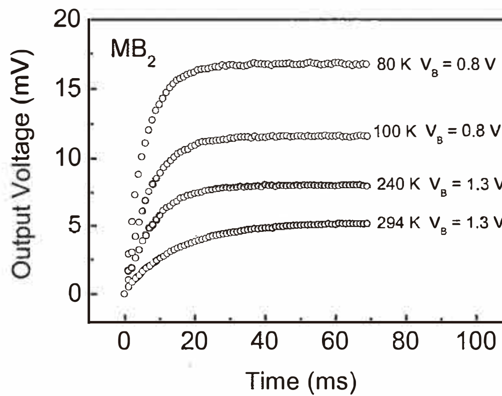

Fig. 4. Output voltage of the bridge for the MB_2 at various substrate temperatures. The measurement was carried out at 80 K, 100 K, 120 K, 150 K, 180 K, 205 K, 240 K, 270 K and 294 K and only a subset is shown for clarity.

T_s, and its magnitude can be estimated[11] from the formula $G_{rad} \sim 4\varepsilon A\sigma T_s^3$, where A is the surface area of the membrane, ε is the emissivity of the membrane and σ is the Stephan-Boltzmann constant. For the 110×160 mm^2 microbolometers used in the study, the radiation-limited thermal conductance at room temperature (294 K) is approximately 2×10^{-7} W/K assuming 50% emissivity. This is of the same order of magnitude as the thermal conductivity via the legs of MB_1 at 250 K. The change of thermal conductance in the entire temperature range was found to be less than a factor of two due to conduction through the legs. However, with increasing temperature, the radiation component becomes the dominant heat-loss mechanism for MB_1. This was not the case for MB_2 since it has thermal conductance nearly an order of magnitude higher through the legs. This observation suggests that the operating temperature plays an important role in determining the ultimate sensitivity of microbolometer-based infrared detectors.

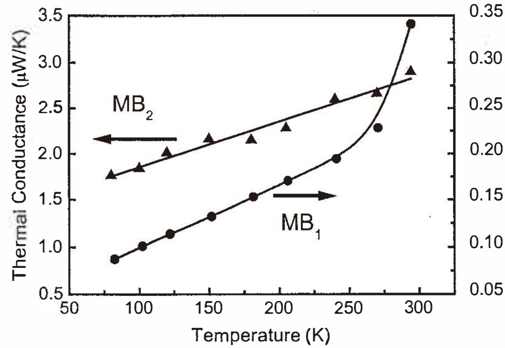

Fig. 5. Variation of thermal conductance with substrate temperature for MB_1 and MB_2. The contribution of the heat loss through radiation is clearly evident in MB_1 at higher substrate temperatures.

In addition to the thermal conductance, the thermal masses of the two microbolometers were also estimated as a function of temperature using the measurements and eq. (4). Figure 6 shows that the thermal mass of the two microbolometers increases linearly with temperature. Since the material volume of the two membranes is nearly the same, the thermal masses of the microbolometers were found to be close to each other as expected. The linear dependence of the thermal mass with temperature is mainly due to the linear increase of the specific heat capacity of the PECVD silicon nitride membrane for temperatures below the Debye temperature[12] ($\Theta_D > 1000$ K for silicon nitride). The thermal mass, increased by a factor of five over the temperature interval used, is significantly higher than the increase in thermal conductance through the legs (less than a factor of two). This implies that thermal time constant (H/G) increases with increasing temperature which can affect the operating speed of thermal imagers at elevated temperatures.

5. Conclusions

The effect of varying the operating temperature (80–294 K) on the electrical and thermal parameters of microbolometer infrared detectors with Ti resistive sensor elements was studied. The parameters studied included the temperature coefficient of resistance (TCR), thermal conductance and thermal mass. Measurements showed that the thermal mass increases linearly with operating temperature while the thermal conductance has a linear dependence below 250 K and then rapidly increases depending on the thermal conductance through the legs. The rapid increase of thermal conductance is mainly due to the radiated heat loss, which may limit the performance of the microbolometer sensors at high ambient temperatures. The faster increase of thermal mass compared to thermal conductance implies that the thermal time constant of the bolometer increases with temperature. These variations are particularly important for the design of uncooled infrared cameras operating without a thermoelectric (TE) temperature stabilizer.

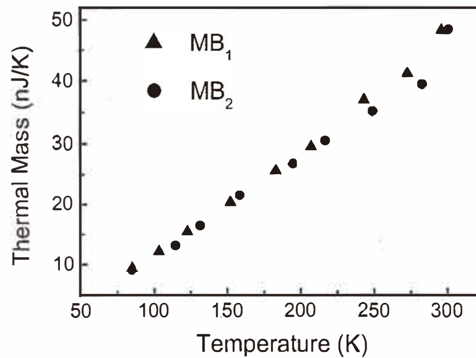

Fig. 6. Variation of thermal mass with substrate temperature for MB_1 and MB_2.

Acknowledgments

The authors would like to thank U. Sridhar, W. J. Zeng, G. Chen, T. Mei and P. D. Foo for their invaluable contributions. The work is supported in part by the U. S. Naval Postgraduate School.

References

1 K. C. Liddiard: Infrared Physics **26** (1986) 43.
2 R. A. Wood, C. J. Han and P. W. Kruse: IEEE Solid-State and Actuator Workshop Technical Digest 1992 (IEEE, New York, 1992) p. 132.
3 A. Tanaka, S. Matsumoto, N. Tsukamato, S. Itoh, K. Chiba, T. Endoh, A. Nakazato, K. Okuyama, Y. Kumazawa, M. Hijikawa, H. Gotoh, T. Tanaka and N. Teranishi: IEEE Trans. on Electron Devices **143** (1996) 1844.
4 A. D. Oliver and K. D. Wise: Sensors and Actuators A **73** (1999) 222.
5 H. Beratan, C. Hanson and E. G. Meissner: SPIE **2274** (1994) 147.
6 P. G. Datskos, P. I. Oden, T. Thundat, E. A. Wachter, R. J. Warmack and S. R. Hunter: Appl. Phys. Lett. **69** (1996) 2986.
7 X. Gu, G. Karunasiri, G. Chen, U. Sridhar and B. Xu: Appl. Phys. Lett **72** (1998) 1881.
8 P. Eriksson, J. Y. Andersson and G. Stemme: J. Microelectromech. Syst. **6** (1997) 55.
9 C. J. Smithells: Smithells Metals Reference Book (Butterworth Heinemann, New York, 1992) pp 19-1 to 19-3.
10 M. V. S. Ramakrishna, G. Karunasiri, P. Neuzil, U. Sridhar and W. J. Zeng: Sensors and Actuators A **79** (2000) 122.
11 E. L. Dereniak and G. D. Boreman: Infrared Detectors and Systems (John Wiley, New York, 1996) p 400.
12 J. Z. Jiang, H. Lindelov, L. Gerward, K. Stahl, J. M. Recio, P. Mori-Sanchez, S. Carlson, M. Mezouar, E. Dooryhee, A. Fitch and D. J. Frost: Phys. Rev. B **65** (2002) 161202.